

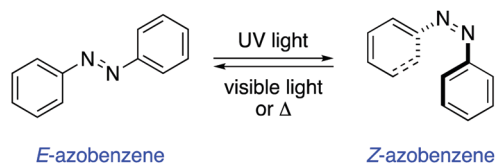
a specific focus on the *E/Z* isomerisation of double bonds¹¹ that are integrated in the structure of the catalyst as the light-triggered event. The discussion has been primarily organised according to the nature of the photoisomerisable double bond. Photoswitchable catalysts based on photochromic units susceptible of photocyclization such as diarylethenes¹² or spiropyranes¹³ will therefore not be discussed.

Azobenzene-based photoswitchable catalysts

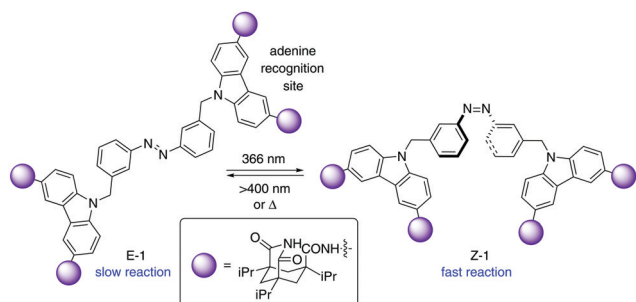
Azobenzenes are among the most studied and well-established photochromic entities.¹⁴ Upon irradiation, the N=N bond undergoes a photoisomerisation from the *E* to the *Z* isomer, which reverts back to the thermodynamically more stable *E* isomer in the dark (Scheme 1). This reverse isomerisation can also be triggered by irradiation with visible light.

Photoswitchable bifunctional catalysts

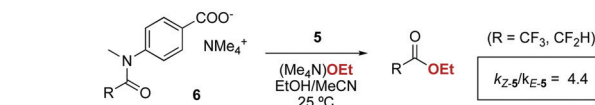
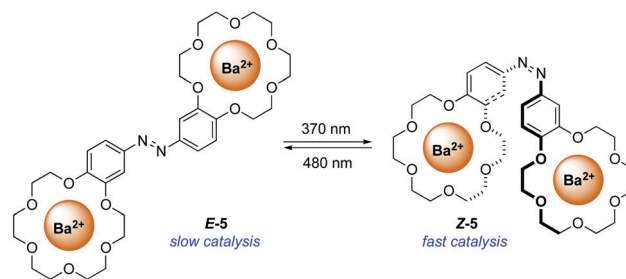
The photoisomerisation of azobenzenes is accompanied by a large geometrical change in the molecule, which in the case of catalytically active species can be exploited for the control of their activity. A pioneer example of a photoswitchable template **1** for cooperative bifunctional catalysis was described by Würthner and Rebek in 1995 utilising two carbazole-based adenine receptors linked by an azobenzene scaffold, which exerted



Scheme 1 Photoisomerisation of azobenzene.



Scheme 2 Photocontrol over amide bond formation between **2** and **3**.



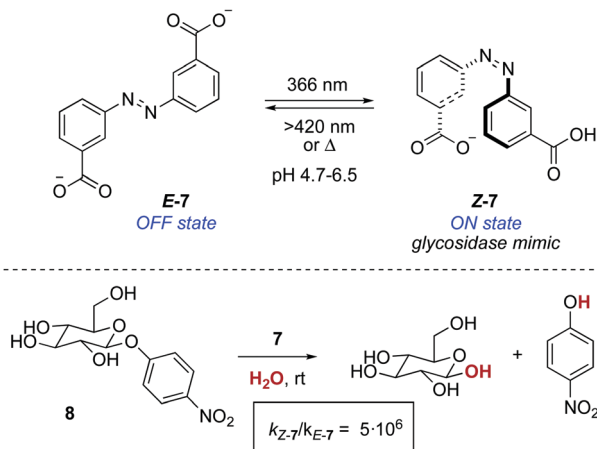
Scheme 3 Photoswitchable catalyst **5** for the ethanolation of **6**.

control over the rate of the amide bond formation to give **4** (Scheme 2).¹⁵ After recognition of the adenine-containing substrates **2** and **3**, the *E*-form of **1** places them apart from each other, which translates into a low reaction rate for the amide bond formation. On the other hand, *Z*-1 brings the two reacting partners into close proximity, which facilitates the coupling reaction as inferred from a significant increase in the reaction rate after irradiation with UV light. Thus, the use of the 50:50 mixture of *E*-1 and *Z*-1 that resulted from irradiation with 366 nm light caused a nearly nine-fold enhancement of the coupling rate. Nonetheless, the product **4** remains bound to **1** after amide bond formation, which precludes its turnover and therefore its task as a photoswitchable catalyst.

The first successful example of a photoswitchable bifunctional catalyst was reported in 2003 by Cacciapaglia and co-workers who, inspired by the pioneer work by Shinkai on photoresponsive crown ethers,¹⁶ developed phototunable cooperative catalyst **5** for the ethanolation of tertiary anilides **6** (Scheme 3).¹⁷ Dinuclear barium complexes of bis-crown ether hosts are known to catalyse the basic ethanolation of tertiary acetanilides through a cooperative process in which one of the barium centres binds the carboxylate moiety of the substrate while the other barium centre activates the nucleophilic ethanoate and delivers it to the carbonyl of the acetanilide.¹⁸ The bis-barium complex of azobenzene-containing bis(benzo-18-crown-6) **5** exhibits low activity towards the ethanolation of anilides **6** when in its *E*-form. In contrast, photoswitching of the azobenzene moiety to its *Z*-form (PSS ratio *Z*-5:*E*-5 = 95:5) turns **5** into a more active catalyst due to the proximity between two barium centres. However, the structural similarities between the reaction product and **6** still result in a notable product inhibition due to competitive coordination.

A photoresponsive bifunctional organocatalyst was later developed based on the cooperative effects of two azobenzene-tethered trityl alcohol functionalities.¹⁹ The enhanced acidity of the *Z* form, which results from an intramolecular hydrogen bond between the two hydroxyl groups, translated into an acceleration of the reaction rate in a phosphine-catalysed Morita-Baylis-Hillman reaction. In a conceptually related approach, the photomodulation of pK_a in an azobenzene-tethered bis-carboxylic acid **7** was the key

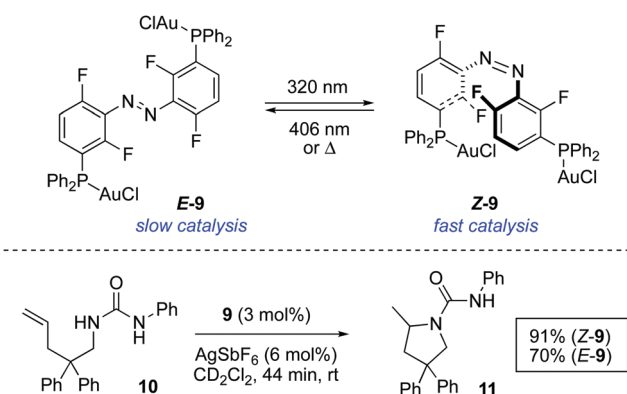
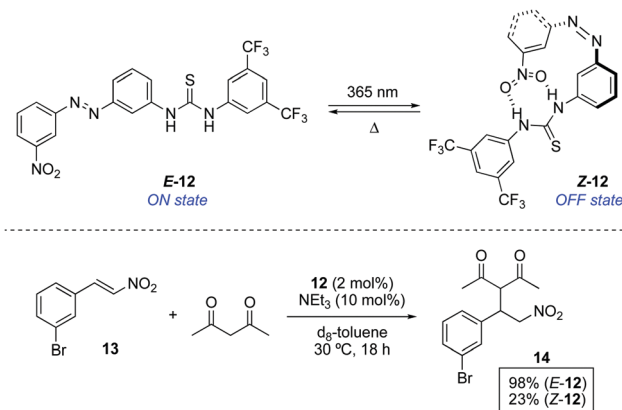


Scheme 4 Photoresponsive glycosidase mimic **7**.

to design a photoresponsive glycosidase mimic (Scheme 4).²⁰ The deprotonation of both carboxylic acid groups in *E*-**7** occurs at the same pH, whereas in *Z*-**7**, which is obtained by irradiation with 366 nm light (PSS ratio *Z*-**7** : *E*-**7** = 70 : 30), this takes place stepwise. Therefore, *Z*-**7** exists between pH 4.7 and 6.5 as the monoanionic species, which parallels the active form of a glycosidase in terms of functionality. Hence, an enhancement in the reaction rate of six orders of magnitude was observed at pH 5.8 for the hydrolysis of 4-nitrophenyl-β-D-glycopyranoside **8** with respect to that of the background reaction.

In a more recent example, the catalytic activity of bimetallic gold(i) complex **9** was modulated by photoisomerisation of the azobenzene linking group (Scheme 5).²¹ Both isomers of **9** could be isolated and tested independently as catalysts. The reaction rate of the intramolecular hydroamination of **10** turned out to be dependent on the configuration of the azobenzene moiety. Thus, *Z*-**9**, which results from the irradiation of *E*-**9** with 320 nm light, exhibits a greater activity and this acceleration is tentatively attributed to a cooperative effect between the two metal centres.

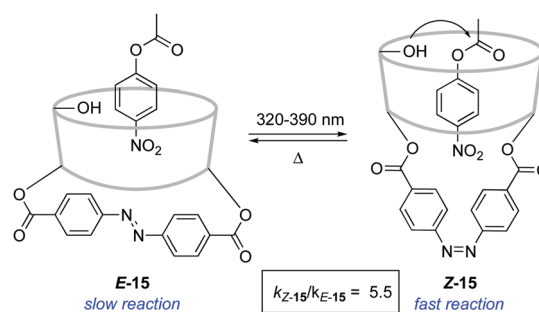
A complementary approach to control the catalytic activity consists of the switchable deactivation of the catalyst by means of intramolecular interactions when two groups are brought

Scheme 5 Photoswitchable bimetallic gold complex **9** and control over the rate of intramolecular hydroamination of **10**.Scheme 6 Photocontrol over the deactivation of organocatalyst **12**.

into close proximity. In this context, organocatalyst **12**, in which a thiourea (hydrogen donor) and a nitro (hydrogen acceptor) groups are linked through an azobenzene bridge, was tested in a thiourea-catalysed nitro-Michael addition (Scheme 6).²² The thiourea reacting site in *E*-**12** is available to efficiently catalyse the addition of acetylacetone to nitrostyrene **13**. On the other hand, the nitro group in *Z*-**12**, which is obtained by irradiation of *E*-**12** with 365 nm light (PSS ratio *Z*-**12** : *E*-**12** = 56 : 44), is placed close enough to the thiourea unit to interact with it thereby blocking the active site. As a result, the activity upon irradiation is notably diminished, albeit not completely suppressed due to the low PSS ratio. When the nitro group was replaced by a methyl group in **12**, the reactivity of *E* and *Z* isomers was not significantly different, which proves that the inhibition derives not only from a steric blocking of the active site but rather from a competitive intramolecular hydrogen bonding event. In a similar vein, **12** was later used as a photoswitchable catalyst in the ring-opening polymerization of lactide.²³

Photoswitchable catalysis by regulation of steric effects

An alternative strategy to regulate the activity of a catalyst relies on the alteration of the steric bulk around its reaction site. A pioneering example was reported in 1981 for the photo-switchable hydrolysis of *p*-nitrophenylbenzoate catalysed by β-cyclodextrin **15** to which a 4,4'-bis-(carboxy)azobenzene was attached as a capping unit (Scheme 7).²⁴ The change in

Scheme 7 Photocontrol over ester hydrolysis catalysed by azobenzene-capped β-cyclodextrin **15**.

geometry of the azobenzene moiety upon irradiation translates into an alteration of the depth of the hydrophobic pocket of the β -cyclodextrin where the substrate needs to bind prior to hydrolysis. Thus, *E*-15 effectively prevents the binding of the ester substrate in the cavity, which impedes its hydrolysis, whereas the formation of *Z*-15 upon irradiation with 365 nm light resulted in up to a 5-fold increase in the hydrolysis reaction rate when 38% of the *Z* isomer was present. It was subsequently demonstrated that the use of a histidine linker for the attachment of the diazobenzene scaffold enabled photocontrol over a related β -cyclodextrin-catalysed hydrolysis, which was effectively switched by irradiation from an inactive state in the *E*-form to a catalytically active state in the *Z*-form.²⁵

The light-gated modulation of the Brønsted basicity of a conformationally restricted *N*-alkylated piperidine was elegantly realised through the attachment of a bulky azobenzene fragment.²⁶ The basic centre in **16** can be reversibly shielded by photoisomerisation of the azobenzene moiety, which was used to control the reaction rate in a base-catalysed Henry reaction (Scheme 8). The lone pair of the piperidine nitrogen is surrounded by the bulky aromatic fragment in the thermodynamically more stable *E*-form, which hinders its reactivity. Irradiation with 365 nm light generates *Z*-16 (PSS ratio *Z*-16:*E*-16 > 95:5), in which the active site becomes accessible. Azobenzene **16** proved to be a suitable photoswitchable catalyst for the reaction between *p*-nitrobenzaldehyde and nitroethane, where the isomerisation from *E*-16 to *Z*-16 resulted in a more than 35-fold increase in the rate of formation of **17**. In a more recent study, the hydrogen bond formation ability of **16** was monitored in the infrared spectral range using MeOH as the hydrogen donor, which was used as a probe of the accessibility to the active site of the catalyst.²⁷ The force generated by the azobenzene in the isomerisation process is enough to extrude MeOH from the active site within just a few picoseconds, thereby preventing access to the binding site. A related switchable piperidine base was also immobilised on silica gel,²⁸ although its use as a catalyst has not yet been described.

In a conceptually related study, the immobilization of a proline catalyst onto the surface of a gold nanoparticle through an azobenzene linker has been recently utilised to reversibly photocontrol the rate of the aldol reaction between cyclohexanone

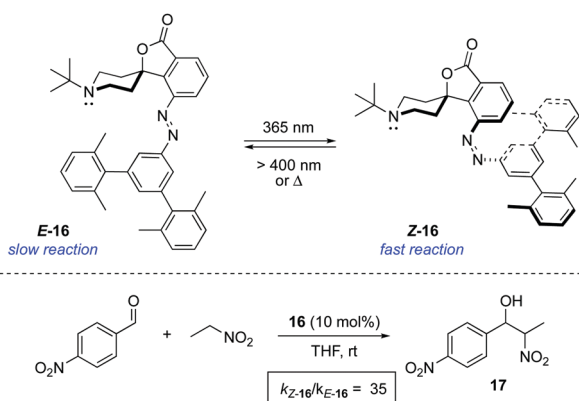
and *p*-nitrobenzaldehyde.²⁹ The photoregulation was based on the active site being buried or exposed to the reaction mixture depending on the configuration of the azobenzene functionality.

Azobenzenes have also been incorporated in phosphine ligands to control the catalytic activity of the corresponding metal complexes. Thus, the differences in geometry derived from the photoinduced isomerisation of an azobenzene-linked Rh(I)-bisphosphine complex were used to gain photocontrol over the rate of hydrogenation of CO₂, which is attributed to the change in the bite angle of the bisphosphine ligand.³⁰ In addition, the photocontrolled generation of hydrogen by hydrolytic decomposition of ammonia-borane was achieved using a ruthenium(II) half-sandwich complex bearing an azobenzene-containing phosphine ligand.³¹

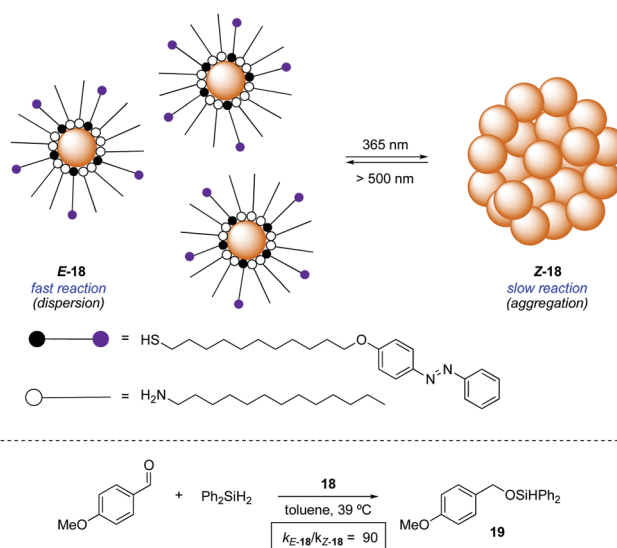
Photoswitchable aggregation state

An alternative approach to control the catalytic activity relies on the regulation of the aggregation/dispersion of catalytically active species. This concept was first realised for the hydrosilylation of *p*-anisaldehyde with diphenylsilane catalysed by Au nanoparticles **18** decorated with a mixed self-assembled monolayer of dodecylamine and azobenzene-terminated alkane thiols (Scheme 9).³² The nanoparticles remain dispersed in the absence of light (*E*-18) and aggregate upon UV light irradiation (*Z*-18). Thus, the exposed surface area gets significantly reduced in the presence of UV light and, as a consequence, the reaction rate for the formation of **19** gets dramatically lower. Irradiation with visible light regenerates the dispersed state and therefore restores the activity of the Au nanoparticles. This modulation of activity could be repeated up to three times.

In a different design, the modulation of the activity of a pyridyl-containing bisamide catalyst **20** was achieved through the light-triggered isomerisation of the attached azobenzene functionality, which had a direct influence on its aggregation

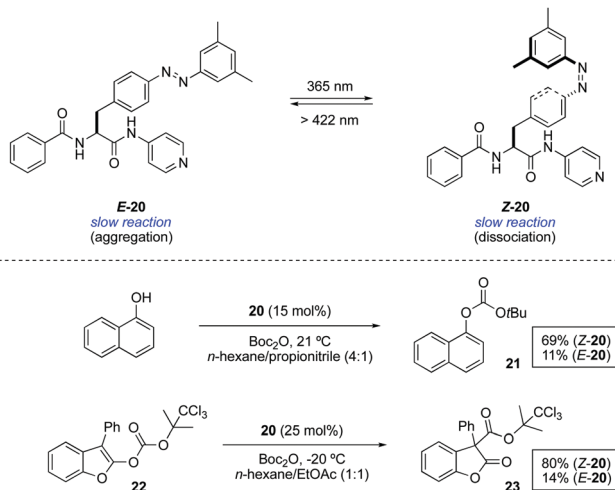


Scheme 8 Photoswitchable base **16** and its activity in a Henry reaction.



Scheme 9 Photoswitchable aggregation of Au nanoparticles **18**.



Scheme 10 Photoswitchable aggregation of **20**.

state (Scheme 10).³³ The catalyst in its *E*-form formed aggregates in a mixture of hexane/propionitrile 4 : 1, which were dissociated upon irradiation with UV light leading to a homogeneous solution due to the disruption of intermolecular hydrogen bonds (PSS ratio *Z*-**20** : *E*-**20** = 96 : 4). The influence of the aggregation state of **20** was examined in the context of two transformations that are known to be catalysed by a nucleophilic base. The reaction of 1-naphthol with Boc_2O barely gave rise to 11% of the protected naphthol **21** in the presence of 15 mol% of *E*-**20** at room temperature after 3 h, whereas under the same reaction conditions using *Z*-**20** the reaction proceeded smoothly to form the product in 69% yield. Likewise, the rearrangement of 2-acyloxybenzofuran **22** afforded 3-acyl-2-benzofuranone **23** in 80% yield in the presence of *Z*-**20**, while only 14% of this product was obtained in the presence of aggregated catalyst *E*-**20**. Nonetheless, this difference in activity is restricted to reactions carried out in solvents in which the difference in solubility between the *Z* and *E* forms is large, otherwise similar results are obtained irrespective of the catalyst state.

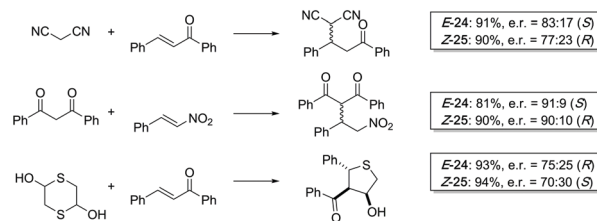
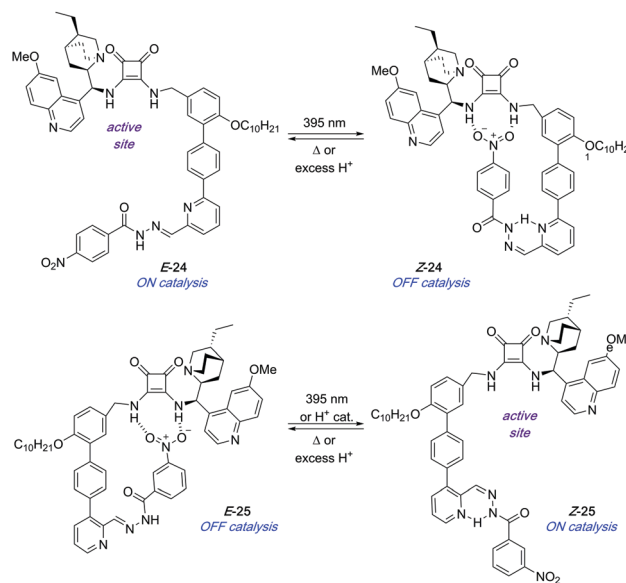
The catalytic activity of a palladium complex of a water-soluble azobenzene-containing phosphane ligand could also be regulated by means of UV irradiation as a result of the different types of aggregates that are formed in the aqueous phase as a function of the azo-benzene geometry.³⁴ This was applied to regulate the rate of the palladium-catalysed cleavage of allyl-undecyl-carbonate in a heptane/water biphasic reaction medium.

Hydrazone-based photoswitchable catalysts

Despite the growing interest in photoswitchable systems based on the isomerisation of $\text{C}=\text{N}$ bonds experienced over the last decade, both using imines³⁵ and hydrazones³⁶ as the photochromic entities, their applications in photoswitchable catalysis still remain scarce.

In 2017, a pair of enantioselective switchable organocatalysts **24** and **25** were developed based on a pyridyl-acyl

hydrazone scaffold as the photoisomerisable moiety (Scheme 11).³⁷ The active site in both catalysts is a bifunctional cinchona alkaloid-squaramide motif, which is able to catalyse Michael additions in an enantioselective fashion. On the other hand, a nitrobenzene hydrogen bond acceptor was linked through the photoswitchable hydrazone. In the case of **24**, irradiation with UV light brings the nitro group into close proximity to the squaramide motif, which deactivates the catalyst as a result of intramolecular hydrogen bond interactions. In contrast, a change in the regiochemistry of the pyridine ring in **25** makes the same stimulus trigger the formation of the active species by placing the nitro group far apart from the squaramide centre. The PSS *E* : *Z* ratio reached after irradiation of *E*-**24** and *E*-**25** was in both cases 21 : 79. Nevertheless, in the case of **25** this ratio could be further improved up to 5 : 95 by treatment with substoichiometric amounts of trifluoroacetic acid, which was on the other hand not effective to switch **24** off. Catalysts *E*-**24** and *Z*-**25** efficiently generate opposite enantiomers in several conjugate additions such as the addition of malonitrile, masked thiol, or 1,3-dicarbonyl compounds to chalcone derivatives and β -nitrostyrene with good conversions and levels of stereoselectivity (up to 90% ee using *E*-**24** and 86% ee with *Z*-**25**). Unfortunately, the pair of complementary catalysts cannot operate simultaneously in the same reaction vessel in order to access one or the other enantiomer on demand. It appears that the ON state of one catalyst binds to the OFF state of the other therefore preventing any catalysis.

Scheme 11 A complementary pair of hydrazone-based photoswitchable organocatalysts **24** and **25**.

Stilbene-based photoswitchable catalysts

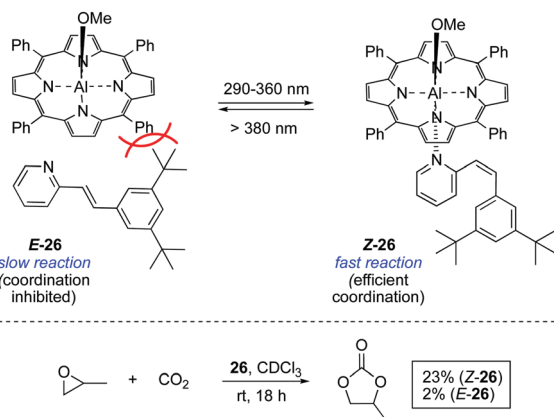
Stilbenes, which undergo *E-Z* isomerisation around the C=C bond upon irradiation, are a well-established and historically relevant class of photoswitches.³⁸ Unlike *Z*-azobenzenes, *Z*-stilbenes can undergo irreversible oxidative electrocyclic to generate phenanthrene-based systems, which is one of the key factors to be taken into account in the design of functional light-driven stilbene-based switchable systems.

Activity control

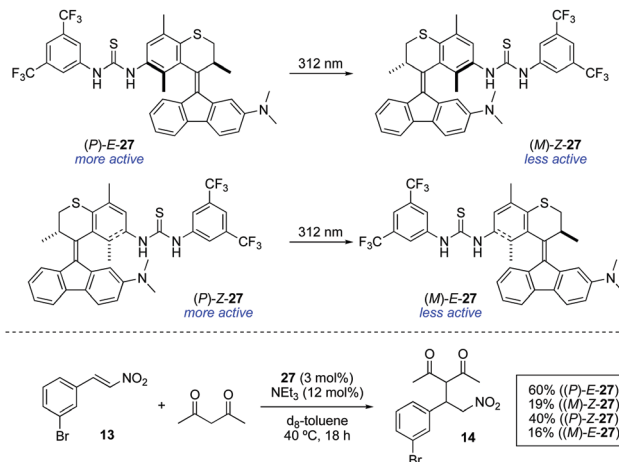
A seminal study in the area was reported in 1999 by Inoue and co-workers, who achieved the light-controlled fixation of CO₂ mediated by aluminium porphyrin **26** (Scheme 12).³⁹ The activity of this system is dependent on the coordination of a bulky 2-stilbazole to the aluminium centre, which can only occur in its *Z* configuration. Once the pyridine moiety is coordinated to the aluminium centre, the resulting complex accelerates the formation of propylene carbonate from propylene oxide and CO₂.

The bis-barium complex of a stilbene-tethered bis-crown ether analogue to **5** was also developed and its activity triggered by irradiation of the *E* isomer with UV light.⁴⁰ However, once activated, it was not possible to revert the complex to its *E* configuration and therefore this system did not fulfil the reversibility requirement for a photoswitchable catalyst.

Bifunctional molecular photoswitches based on the overcrowded alkene scaffold found in the so-called second generation molecular motors⁴¹ have been recently investigated as light-responsive catalysts.⁴² Photoresponsive thioureas **27** were synthesised in both *E* and *Z* forms, which showed efficient photoisomerisation upon irradiation with 312 nm light (Scheme 13). However, the photogenerated metastable states (*M*)-*Z*-**27** and (*M*)-*E*-**27** did not show reversible photoisomerisation upon irradiation with 365 nm light as happens in the unfunctionalised counterparts.³⁸ Furthermore, they both turned out to be ineffective catalysts for the Morita–Baylis–Hillman reaction between 2-cyclohexen-1-one and 3-phenylpropionaldehyde



Scheme 12 A photoswitchable coordination of stilbazole to a porphyrin to form catalyst **26**.



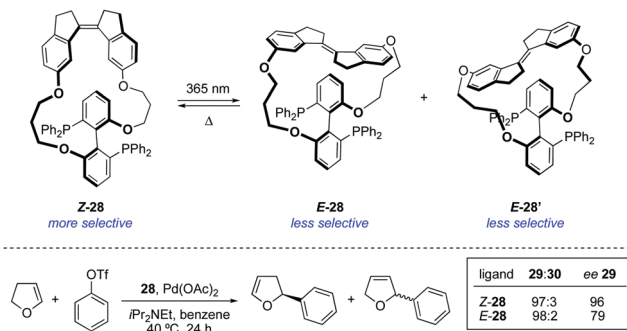
Scheme 13 Light-triggered deactivation of thiourea catalysts **27**.

regardless of the configuration of the double bond, presumably due to the limited catalytic activity of the dimethylaniline moiety. Nonetheless, it was found that the catalytically active thiourea group was deactivated upon irradiation. In order to examine this phenomenon in detail, the addition of acetylacetone to **13** was chosen as a model reaction. In the absence of any catalyst, only 10% conversion was obtained after 18 h. In the presence of (*P*)-*E*-**27**, an increase in the reaction rate was observed, achieving 60% conversion under otherwise identical conditions. In contrast, when metastable form (*M*)-*Z*-**27**, obtained by irradiation with 312 nm light (PSS ratio (*M*)-*Z*-**27** : (*P*)-*E*-**27** = 80:20), was used, the rate of the reaction was significantly decreased to afford **14** in only 19% after 18 h. Contrary to the expectations based on previously described azobenzene-based photoswitchable thiourea catalysts,²² the use of (*P*)-*Z*-**27** under the same reaction conditions led to the formation of **14** in 40% yield. Thus, the lower activity of (*M*)-*Z*-**27** compared to (*P*)-*E*-**27** cannot be simply attributed to a deactivation by intramolecular hydrogen bonding between the thiourea and the dimethylamino groups as in the case of **12**, since this would also be applicable to some extent in the case of (*P*)-*Z*-**27**. Irradiation with 312 nm light led, as in the previous case, to the formation of a less active species, (*M*)-*E*-**27**, which again points towards a deactivation mechanism different from simple shielding of the reactive site as in the case of **16**.²⁶ The rationale for the deactivation of **27** upon irradiation remains to this point unclear and further studies are still necessary in order to apply these systems as ON/OFF photoswitchable catalysts.

Stereoselectivity control

The attachment of a stiff-stilbene photoswitch to the backbone of a chiral biaryl bisphosphine ligand **28** enabled control over the stereochemical outcome of several palladium-catalysed transformations (Scheme 14).⁴³ The irradiation of *Z*-**28** with UV light (365 nm) induced the formation of two different *E*-**28** diastereoisomers, which could be isolated by column chromatography and tested independently as ligands in palladium-catalysed asymmetric Heck

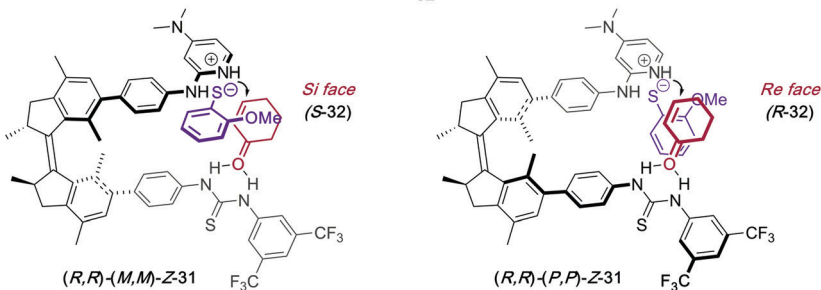
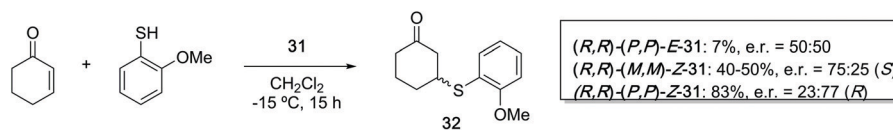
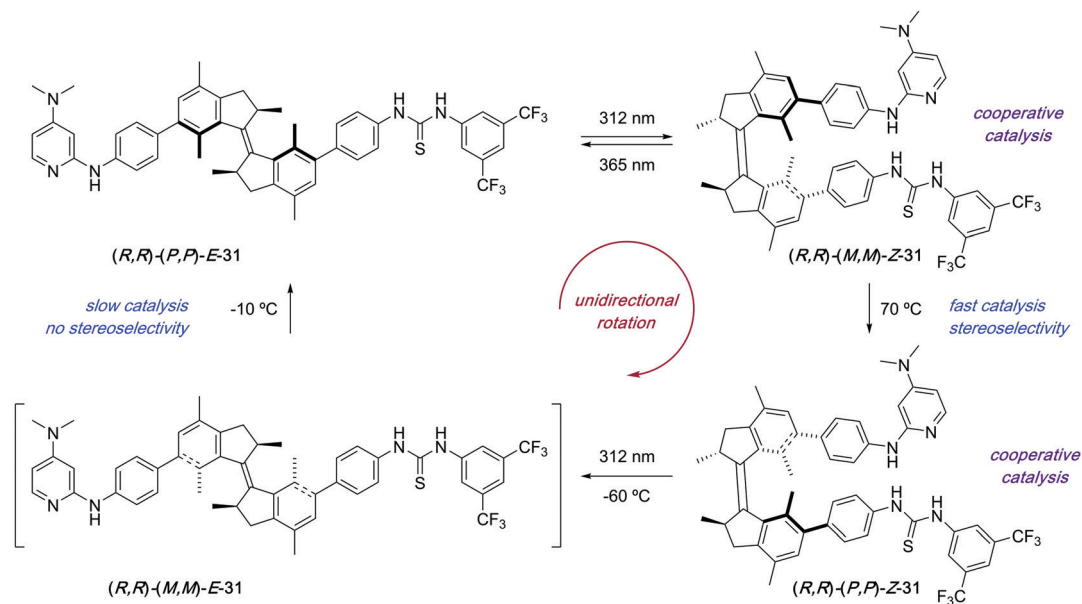


Scheme 14 Photoresponsive biaryl bis(phosphine) ligand **28**.

reaction and Trost allylic alkylations. The enantioselectivities achieved in the presence of *Z*-**28** were in all cases higher than with *E*-**28**, though the same enantiomer was always favoured.

The first example of stereodivergent photoswitchable catalysis was reported in 2011 by our group utilising a unidirectional first generation light-driven molecular motor⁴⁴ as the

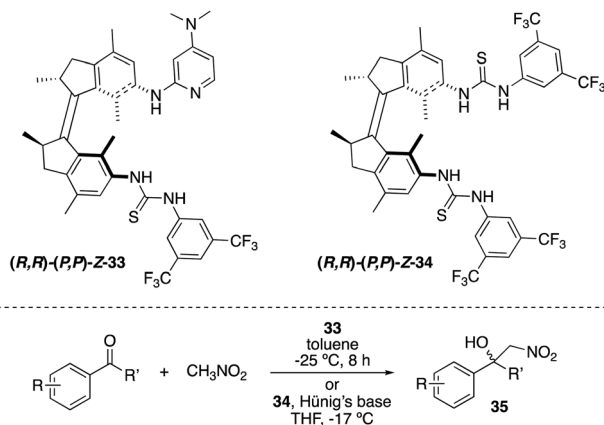
photoresponsive core of the catalyst,⁴⁵ which allowed for the sequential regulation of both the catalytic activity and the stereochemical outcome of a thia-Michael addition through application of the appropriate stimulus. The designed chiral motor-based organocatalyst **31** contains a thiourea functionality and a *N,N*-dimethyl-4-aminopyridine (DMAP) Brønsted base,⁴⁶ which can cooperatively catalyse the conjugate addition of thiols to enones (Scheme 15). Unlike the majority of photoswitches, which are bistable, molecular motors based on overcrowded alkenes such as **31** can exist in four different isomeric forms, and this will dictate the relative orientation of the two catalytic moieties. Irradiation of (*P,P*)-*E*-**31** (312 nm) induces the *E*-*Z* isomerisation to generate quantitatively the metastable (*M,M*)-*Z*-**31** isomer, which upon heating at 70 °C can be converted into thermodynamically more stable (*P,P*)-*Z*-**31**. This isomer was purified by preparative HPLC prior to its use as a catalyst. Subsequent irradiation of (*P,P*)-*Z*-**31** (312 nm) generates transient (*M,M*)-*E*-**31**, which readily isomerises back to (*P,P*)-*E*-**31** even at low temperatures. Therefore, three isomeric states, namely (*P,P*)-*E*-**31**, (*M,M*)-*Z*-**31**, and (*P,P*)-*Z*-**31**, are

Scheme 15 Control of stereoselectivity in a thia-Michael reaction using molecular motor **31**.

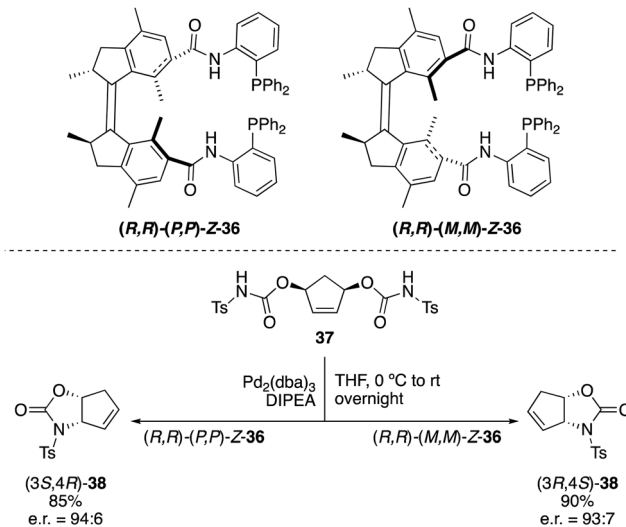
in practice sufficiently stable to be employed as chiral catalysts. When the *(P,P)*-**E-31** isomer was used, the thiourea and DMAP groups were far apart, which precluded any cooperative effect between them. As a result, **32** was formed slowly (7% in 15 h) and obtained as a racemate. On the other hand, the catalytic sites are close enough to act cooperatively in both *Z* configurations of **31**, which resulted in high activity in the formation of **32**. Moreover, *(M,M)*-**Z-31** and *(P,P)*-**Z-31** promoted the preferential formation of opposite enantiomers due to their opposite helicity. Hence, the coordination of the enone and thiol substrates to *(R,R)*-**(M,M)**-**Z-31** favoured the addition to the *Si*-face of the prochiral enone, which resulted in the preferential formation of *S*-**32** (e.r. = 75 : 25), while *R*-**32** was the major enantiomer in the presence of *(R,R)*-**(P,P)**-**Z-31** as a result of the addition to the *Re*-face of the enone (e.r. = 23 : 77). The choice of one or the other enantiomer of the motor catalyst **31** can also be used to control the sequential order of formation of the enantiomers of **32** (*(R,S)*-*(R)*-*(S)* versus *(R,S)*-*(S)*-*(R)*).

A related light-responsive organocatalyst **33** lacking the phenyl spacer between the catalytic sites and the molecular motor core proved to be effective in exerting stereocontrol over the Henry reaction between nitromethane and α,α,α -trifluoromethylketones (Scheme 16).⁴⁷ As in the case of **31**, *E*-**33** exhibited low activity, whereas *(M,M)*-**Z-33** and *(P,P)*-**Z-33** afforded preferentially opposite enantiomers of the products **35** (e.r. up to 86 : 14 for *(R)*-**35** versus 21 : 79 for *(S)*-**35**). It was subsequently demonstrated that it is not required to have the basic functional group attached to the motor.⁴⁸ Thus, bisurea motor **34** was used for the stereo-divergent Henry reaction using substoichiometric amounts of Hünig's base. The corresponding nitroalcohols **35** were obtained in up to 88 : 12 e.r. (*S*-**35**) in the presence of *(M,M)*-**Z-34** and 80 : 20 (*R*-**35**) when *(P,P)*-**Z-34** was used as the catalyst.

Not only switchable organocatalysts but also ligands for metal catalysis can be prepared based on first generation molecular motors. A bisphosphine ligand **36**, reminiscent of Trost ligands,⁴⁹ was obtained by linkage of the diphenylphosphine moieties to the motor core *via* an amide tether (Scheme 17).⁵⁰ This ligand, which exhibited a rotational behaviour similar to that of **31**, proved to be



Scheme 16 Light- and heat-responsive thiourea catalysts **33** and **34** for the stereocontrol over the Henry reaction.

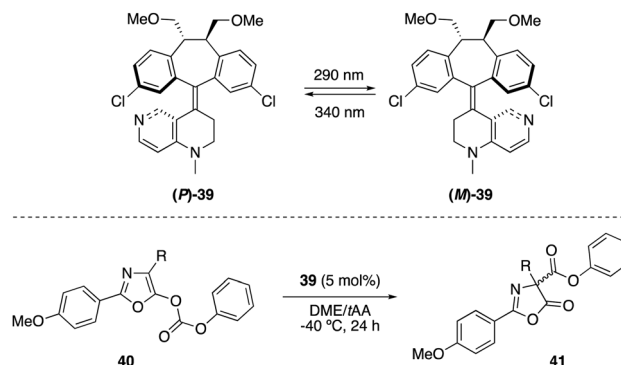


Scheme 17 Palladium-catalysed desymmetrisation using molecular motor **36** as the ligand.

effective in the palladium catalysed intramolecular desymmetrisation of *meso*-biscarbamate **37**. Thus, *(3S,4R)*-**38** was obtained in the presence of *(P,P)*-**Z-36** (e.r. = 94 : 6), whereas the use of *(M,M)*-**Z-36** provided preferentially the opposite enantiomer *(3R,4S)*-**38** (e.r. = 93 : 7) under identical reaction conditions.

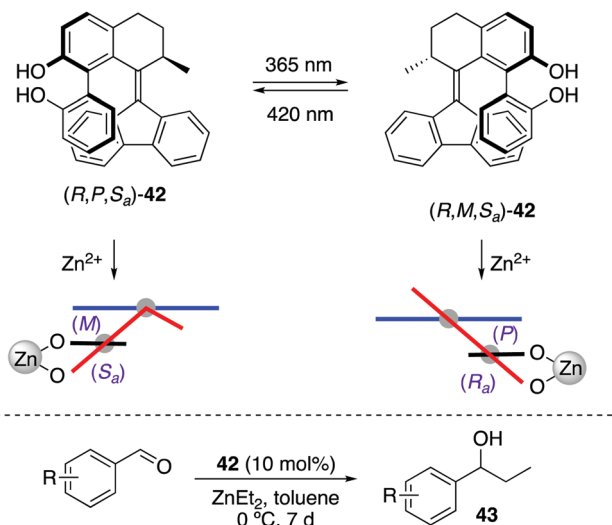
Optically switchable dibenzosuberane-based helicene **39**, which contains a 4-*N*-methylaminopyridine subunit, was later established as an efficient enantiodivergent catalyst for the Steglich rearrangement of *O*-carboxylazlactones **40** (Scheme 18).⁵¹ The two pseudoenantiomers *(P)*-**39** and *(M)*-**39** could be repeatedly interconverted by irradiation at two different wavelengths. Hence, irradiation with 290 nm converted *(P)*-**39** into *(M)*-**39** (PSS ratio *(M)*-**39** : *(P)*-**39** > 99 : 1), while the latter could be reverted to *(P)*-**39** with 340 nm light (PSS ratio *(M)*-**39** : *(P)*-**39** = 9 : 91). The rearranged products **41** were obtained in up to 91% (*R*) and 94% (*S*) ee using *(P)*-**39** and *(M)*-**39**, respectively.

Recently, a photoresponsive bis(2-phenol)-substituted photo-switch **42** was built based on the core of second generation molecular motors (Scheme 19).⁵² This design enables a dynamic central-helical-axial transfer of chirality in which the preferential



Scheme 18 Enantiodivergent Steglich rearrangement using photoswitchable catalyst **39**.





Scheme 19 Central-helical-axial transfer of chirality in **42** and its application in stereodivergent addition of ZnEt_2 to aromatic aldehydes.

chirality of the biaryl motif is coupled to the reversible photo-switching of the helicity of the motor core upon irradiation, which is dictated by the configuration of the stereogenic centre adjacent to the overcrowded alkene axis. Thus, (R,P,S_a) -**42** and (R,M,S_a) -**42** can be interconverted by irradiation with 365 nm (PSS ratio = 17:83) and 420 nm light (PSS ratio = 50:50), respectively, which was used to control the stereochemical outcome of the addition of diethylzinc to aromatic aldehydes. The enantioselectivity of this process was successfully reversed upon irradiation, giving rise preferentially to *R*-**43** in the presence of (R,P,S_a) -**42** (up to 68% ee) and *S*-**43** after irradiation with 365 nm light (up to 55% ee).

Conclusions and outlook

The emergent field of photoswitchable catalysis has experienced over the past 20 years a remarkable progress through the advent of light-responsive switches and molecular machines with increased levels of sophistication. The judicious choice of a photochromic unit and its precise incorporation into the structure of a catalyst offers unparalleled opportunities to control in a non-invasive way its activity and/or selectivity with exquisite spatio-temporal precision. However, there are still several unresolved challenges that need to be addressed in order to turn the field from a proof of concept into a practical tool in synthesis.

A number of photoswitchable homogeneous catalysts have been successfully developed by implementing azobenzene, hydrazone, or stilbene motifs into the catalyst structure. Furthermore, the immobilization of photoswitchable scaffolds onto the surface of catalytically active nanoparticles has also been realised. The majority of the reported examples target the ON/OFF control of the activity of the catalyst through a light-triggered geometrical change in its structure. More recently, the use of chiral stilbene-based overcrowded alkenes has enabled the development of photoswitchable stereodivergent catalysts able to exert dual stereocontrol on chemical transformations,

which is particularly desirable from the perspective of pharmaceutical industry. This concept would allow for the on-demand preparation of the stereoisomer of interest starting from a single isomer of the catalyst, which could lead to more versatile and efficient processes. Nonetheless, these examples still remain scarce and further investigations will be required in order to demonstrate their generality. In general, most of the examples reported to date do not comprehensively analyse how the differences in catalytic activity are affected over several photoswitching cycles. Furthermore, the *in situ* regulation of the catalytic activity, which could be of particular interest to control multitasking catalysts or reactions in flow, often remains a challenge despite the high spatiotemporal resolution of light, and preirradiation of the catalyst is frequently required. Fully compatible photoswitchable catalysts that are able to on-demand catalyse two different orthogonal reactions, which has been recently accomplished with a pH-responsive rotaxane-based molecular machine,⁵³ also remain a challenge in the field. In addition, the use of (photo)switchable catalysts for the regulation of tacticity, chain length and/or topology in polymers may lead to new classes of materials with unprecedented properties.⁵⁴

Despite the field of photoswitchable catalysis is still at an early stage, the outstanding advances herein described set the basis for further investigations towards more robust, multi-functional, and broadly applicable light-responsive catalysts. The growth of the field of molecular machines combined with the progress achieved in metal catalysis, organocatalysis, and supramolecular chemistry holds great potential for the development of new generations of (photo)responsive catalysts able to perform complex sequences of tasks or show on command adaptive behaviour in the near future.

Conflicts of interest

There are no conflicts to declare.

Acknowledgements

Financial support from the Ministry of Education, Culture and Science (Gravitation Program 024.001.035), the Ramón Areces Foundation (Postdoctoral fellowship to R. D.), and the European Research Council (Advanced Investigator Grant No. 694345 to B. L. F.) are gratefully acknowledged.

References

- (a) J. Hagen, *Industrial Catalysis: A Practical Approach*, Wiley-VCH, Weinheim, 2nd edn, 2006; (b) H. U. Blaser and E. Schmidt, *Asymmetric Catalysis on Industrial Scale*, Wiley-VCH, Weinheim, 2004.
- (a) *Catalysis: From Principles to Applications*, ed. M. Beller, A. Renken and R. A. van Santen, Wiley-VCH, Weinheim, 2012; (b) J. F. Hartwig, *Organotransition Metal Chemistry: From Bonding to Catalysis*, University Science Books, New York, 2010.
- (a) E. Kuah, S. Toh, J. Yee, Q. Ma and Z. Gao, *Chem. – Eur. J.*, 2016, 22, 8404; (b) J. Meeuwissen and J. N. H. Reek, *Nat. Chem.*, 2010, 2, 615; (c) M. D. Nothling, Z. Xiao, A. Bhaskaran, M. T. Blyth, C. W. Bennett, M. L. Coote and L. A. Connal, *ACS Catal.*, 2019,



- 9, 168; (d) M. T. Reetz, *Adv. Catal.*, 2006, **49**, 1; (e) F. H. Arnold, *Angew. Chem., Int. Ed.*, 2018, **57**, 4143.
- 4 T. W. Traut, *Allosteric Regulatory Enzymes*, Springer, New York, 2008.
- 5 (a) *Molecular Devices and Machines: Concepts and Perspectives for the Nanoworld*, ed. V. Balzani, A. Credi and M. Venturi, Wiley-VCH, Weinheim, 2008; (b) W. R. Browne and B. L. Feringa, *Nat. Nanotechnol.*, 2006, **1**, 25; (c) *Molecular Switches*, ed. W. R. Browne and B. L. Feringa, Wiley-VCH, Weinheim, 2nd edn, 2011; (d) *The Nature of the Mechanical Bond: From Molecules to Machines*, ed. C. J. Brunz and J. F. Stoddart, Wiley-VCH, 2016; (e) S. Erbas-Cakmak, D. A. Leigh, C. T. McTernan and A. L. Nussbaumer, *Chem. Rev.*, 2015, **115**, 10081; (f) A. S. Lubbe, T. van Leeuwen, S. J. Wezenberg and B. L. Feringa, *Tetrahedron*, 2017, **73**, 4837; (g) T. van Leeuwen, A. S. Lubbe, P. Štacko, S. J. Wezenberg and B. L. Feringa, *Nat. Rev. Chem.*, 2017, **1**, 0096.
- 6 For recent reviews on switchable catalysis, see: (a) V. Blanco, D. A. Leigh and V. Marcos, *Chem. Soc. Rev.*, 2015, **44**, 5341; (b) M. Vlatković, B. S. L. Collins and B. L. Feringa, *Chem. – Eur. J.*, 2016, **22**, 17080; (c) J. Choudhury, *Tetrahedron Lett.*, 2018, **59**, 487; (d) J. Choudhury and S. Semwal, *Synlett*, 2018, 141; (e) G. Romanazzi, L. Degennaro, P. Mastroilli and R. Luisi, *ACS Catal.*, 2017, **7**, 4100; (f) L. van Dijk, M. J. Tilby, R. Szpera, O. A. Smith, H. A. P. Bunce and S. P. Fletcher, *Nat. Rev. Chem.*, 2018, **2**, 0117.
- 7 For selected examples, see: (a) S. L. Balof, S. J. P'Pool, N. J. Berger, E. J. Valente, A. M. Shiller and H.-J. Schanz, *Dalton Trans.*, 2008, 5791; (b) V. Blanco, A. Carlone, K. D. Hänni, D. A. Leigh and B. Lewandowski, *Angew. Chem., Int. Ed.*, 2012, **51**, 5166; (c) S. Semwal and J. Choudhury, *Angew. Chem., Int. Ed.*, 2017, **56**, 5556.
- 8 For selected examples, see: (a) I. M. Lorkovic, R. R. Duff and M. S. Wrighton, *J. Am. Chem. Soc.*, 1995, **117**, 3617; (b) C. S. Slone, C. A. Mirkin, G. P. A. Yap, I. A. Guzei and A. L. Rheingold, *J. Am. Chem. Soc.*, 1997, **119**, 10743; (c) K. Arumugam, C. D. Varnado, S. Sproules, V. M. Lynch and C. W. Bielawski, *Chem. – Eur. J.*, 2013, **19**, 10866; (d) J. Wei and P. L. Diaconescu, *Acc. Chem. Res.*, 2019, **52**, 415.
- 9 For selected examples, see: (a) Y. Sohtome, S. Tanaka, K. Takada, T. Yamaguchi and K. Nagasawa, *Angew. Chem., Int. Ed.*, 2010, **49**, 9254; (b) R. J. Chew, X.-R. Li, Y. Li, S. A. Pullarkat and P.-H. Leung, *Chem. – Eur. J.*, 2015, **21**, 4800.
- 10 (a) R. S. Stoll and S. Hecht, *Angew. Chem., Int. Ed.*, 2010, **49**, 5054; (b) B. M. Neilson and C. W. Bielawski, *ACS Catal.*, 2014, **4**, 3; (c) R. Göstl, A. Senf and S. Hecht, *Chem. Soc. Rev.*, 2014, **43**, 1982.
- 11 (a) D. Cameron and S. Eisler, *J. Phys. Org. Chem.*, 2018, **31**, e3858; (b) T. Niazov, B. Shlyahovsky and I. Willner, *J. Am. Chem. Soc.*, 2007, **129**, 6374.
- 12 (a) M. Irie, *Chem. Rev.*, 2000, **100**, 1685; (b) D. Sud, T. B. Norsten and N. R. Branda, *Angew. Chem., Int. Ed.*, 2005, **44**, 2019; (c) D. Wilson and N. R. Branda, *Angew. Chem., Int. Ed.*, 2012, **51**, 5431; (d) B. M. Neilson and C. W. Bielawski, *Organometallics*, 2013, **32**, 3121.
- 13 G. Berkovic, V. Krongauz and V. Weiss, *Chem. Rev.*, 2000, **100**, 1741.
- 14 H. M. D. Bandara and S. C. Burdette, *Chem. Soc. Rev.*, 2012, **41**, 1809.
- 15 F. Würthner and J. Rebek, *Angew. Chem., Int. Ed. Engl.*, 1995, **34**, 446.
- 16 (a) S. Shinkai, T. Nakaji, Y. Nishida, T. Ogawa and O. Manabe, *J. Am. Chem. Soc.*, 1980, **102**, 5860; (b) S. Shinkai, T. Nakaji, T. Ogawa, K. Shigematsu and O. Manabe, *J. Am. Chem. Soc.*, 1981, **103**, 111; (c) S. Shinkai, K. Shigematsu, Y. Kusano and O. Manabe, *J. Chem. Soc., Perkin Trans. 1*, 1981, 3279; (d) S. Shinkai, T. Ogawa, Y. Kusano, O. Manabe, K. Kikukawa, T. Goto and T. Matsuda, *J. Am. Chem. Soc.*, 1982, **104**, 1960.
- 17 R. Cacciapaglia, S. Di Stefano and L. Mandolini, *J. Am. Chem. Soc.*, 2003, **125**, 2224.
- 18 R. Cacciapaglia, S. Di Stefano, E. Kelderman and L. Mandolini, *Angew. Chem., Int. Ed.*, 1999, **38**, 348.
- 19 T. Imahori, R. Yamaguchi and S. Kurihara, *Chem. – Eur. J.*, 2012, **18**, 10802.
- 20 M. Samanta, V. S. R. Krishna and S. Bandyopadhyay, *Chem. Commun.*, 2014, **50**, 10577.
- 21 T. Arif, C. Cazorla, N. Bogliotti, N. Saleh, F. Blanchard, V. Gandon, R. Métivier, J. Xie, A. Voituriez and A. Marinetti, *Catal. Sci. Technol.*, 2018, **8**, 710.
- 22 L. Osorio-Planes, C. Rodríguez-Esrich and M. A. Pericàs, *Org. Lett.*, 2014, **16**, 1704.
- 23 Z. Dai, Y. Cui, C. Chen and J. Wu, *Chem. Commun.*, 2016, **52**, 8826.
- 24 A. Ueno, K. Takahashi and T. Osa, *J. Chem. Soc., Chem. Commun.*, 1981, 94.
- 25 W.-S. Lee and A. Ueno, *Macromol. Rapid Commun.*, 2001, **22**, 448.
- 26 (a) M. V. Peters, R. S. Stoll, A. Kühn and S. Hecht, *Angew. Chem., Int. Ed.*, 2008, **47**, 5968; (b) R. S. Stoll, M. V. Peters, A. Kühn, S. Heiles, R. Goddard, M. Bühl, C. M. Thiele and S. Hecht, *J. Am. Chem. Soc.*, 2009, **131**, 357.
- 27 M. Pescher, L. van Wilderen, S. Grützner, C. Slavov, J. Wachtveitl, S. Hecht and J. Breidenbeck, *Angew. Chem., Int. Ed.*, 2017, **56**, 12092.
- 28 R. S. Stoll and S. Hecht, *Org. Lett.*, 2009, **11**, 4790.
- 29 M. Szweczyk, G. Sobczak and V. Sashuk, *ACS Catal.*, 2018, **8**, 2810.
- 30 N. Priyadarshani, B. Ginovska, J. T. Bays, J. C. Linehan and W. J. Shaw, *Dalton Trans.*, 2015, **44**, 14854.
- 31 A. Telleria, P. W. N. M. van Leeuwen and Z. Freixa, *Dalton Trans.*, 2017, **46**, 3569.
- 32 Y. Wei, S. Han, J. Kim, S. Soh and B. A. Grzybowski, *J. Am. Chem. Soc.*, 2010, **132**, 11018.
- 33 A. Nojiri, N. Kumagai and M. Shibasaki, *Chem. Commun.*, 2013, **49**, 4628.
- 34 H. Bricout, E. Banaszak, C. Len, F. Hapiot and E. Monflier, *Chem. Commun.*, 2010, **46**, 7813.
- 35 (a) J.-M. Lehn, *Chem. – Eur. J.*, 2006, **12**, 5910; (b) L. Greb and J.-M. Lehn, *J. Am. Chem. Soc.*, 2014, **136**, 13114; (c) L. Greb, A. Eichhöfer and J.-M. Lehn, *Angew. Chem., Int. Ed.*, 2015, **54**, 14345.
- 36 I. Aprahamian, *Chem. Commun.*, 2017, **53**, 6674.
- 37 G. de Bo, D. A. Leigh, C. R. McTernan and S. Wang, *Chem. Sci.*, 2017, **8**, 7077.
- 38 (a) H. Suzuki, *Bull. Chem. Soc. Jpn.*, 1952, **25**, 145; (b) D. H. Waldeck, *Chem. Rev.*, 1991, **91**, 415.
- 39 H. Sugimoto, T. Kimura and S. Inoue, *J. Am. Chem. Soc.*, 1999, **121**, 2325.
- 40 R. Cacciapaglia, S. Di Stefano and L. Mandolini, *J. Org. Chem.*, 2002, **67**, 521.
- 41 N. Koumura, E. M. Geertsema, M. B. van Gelder, A. Meetsma and B. L. Feringa, *J. Am. Chem. Soc.*, 2002, **124**, 5037.
- 42 S. F. Pizzolato, B. S. L. Collins, T. van Leeuwen and B. L. Feringa, *Chem. – Eur. J.*, 2017, **23**, 6174.
- 43 Z. S. Kean, S. Akbulatov, Y. Tian, R. A. Widenhoefer, R. Boulatov and S. L. Craig, *Angew. Chem., Int. Ed.*, 2014, **53**, 14508.
- 44 N. Koumura, R. W. Zijlstra, R. A. van Delden, N. Harada and B. L. Feringa, *Nature*, 1999, **401**, 174.
- 45 J. Wang and B. L. Feringa, *Science*, 2011, **331**, 1429.
- 46 A. G. Doyle and E. N. Jacobsen, *Chem. Rev.*, 2007, **107**, 5713.
- 47 M. Vlatković, L. Bernardi, E. Otten and B. L. Feringa, *Chem. Commun.*, 2014, **50**, 7773.
- 48 M. Vlatković, J. Volarić, B. S. L. Collins, L. Bernardi and B. L. Feringa, *Org. Biomol. Chem.*, 2017, **15**, 8285.
- 49 B. M. Trost, D. L. van Vranken and C. A. Bingel, *J. Am. Chem. Soc.*, 1992, **114**, 9327.
- 50 D. Zhao, T. M. Neubauer and B. L. Feringa, *Nat. Commun.*, 2015, **6**, 6652.
- 51 C.-T. Chen, C.-C. Tsai, P.-K. Tsou, C.-T. Huang and C.-H. Yu, *Chem. Sci.*, 2017, **8**, 524.
- 52 S. F. Pizzolato, P. Štacko, J. C. M. Kistemaker, T. van Leeuwen, E. Otten and B. L. Feringa, *J. Am. Chem. Soc.*, 2018, **140**, 17278.
- 53 K. Eichstaedt, J. Jaramillo-García, D. A. Leigh, V. Marcos, S. Pisano and T. A. Singleton, *J. Am. Chem. Soc.*, 2017, **139**, 9376.
- 54 (a) N. E. Kamber, W. Jeong, R. M. Waymouth, R. C. Pratt, B. G. Lohmeijer and J. L. Hedrick, *Chem. Rev.*, 2007, **107**, 5813; (b) A. J. Teator, D. N. Lastovickova and C. W. Bielawski, *Chem. Rev.*, 2016, **116**, 1969; (c) F. Eisenreich, M. Kathan, A. Dallmann, S. P. Ihrig, T. Schwaar, B. M. Schmidt and S. Hecht, *Nat. Catal.*, 2018, **1**, 516.

